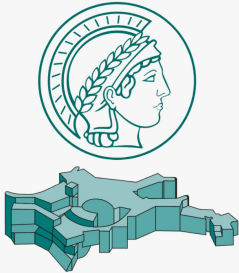


The Cosmic Microwave Background as a window on the Early Universe



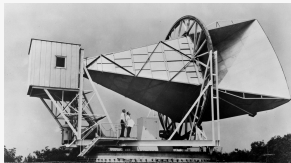
Marta Monelli

Max Planck Institut für Astrophysik
Garching (Germany)

February 22nd, 2023

(accidental) discovery of the CMB

in the 60s, Penzias and Wilson were trying to remove all recognizable interference from their radio antenna, but were left with a residual **noise**.



from *noise* to cosmological signature

our Universe at large scales

in our current understanding, our Universe can be described *on large scales* as being:

- ▶ homogeneous,
- ▶ isotropic,
- ▶ dynamic (expanding).

FRW metric: $ds^2 = -dt^2 + a^2 \delta_{ij} dx^i dx^j$

where a is the *scale factor* and $H \equiv \dot{a}/a$ is called *Hubble parameter*

our Universe at large scales

in our current understanding, our Universe can be described *on large scales* as being:

- ▶ homogeneous,
- ▶ isotropic,
- ▶ dynamic (expanding).

FRW metric:

$$ds^2 = -dt^2 + a^2 \delta_{ij} dx^i dx^j$$
$$= a^2 (-d\eta^2 + \delta_{ij} dx^i dx^j)$$

where a is the *scale factor* and $H \equiv \dot{a}/a$ is called *Hubble parameter*

cosmic dynamics

$$\text{Einstein equations: } G_{\mu\nu} = 8\pi G T_{\mu\nu}.$$

← from FRW metric

→ assuming the Universe to be filled with a fluid ($T_{00} = -\rho$, $T_{ii} = p$)

Friedmann equations:

$$H^2 = \frac{8\pi G}{3}\rho,$$
$$2\dot{H} + 3H^2 = -8\pi Gp.$$

Pressure

Radiation ($\gamma + \nu$): $p_r = \rho_r/3$.

Matter (ordinary + CDM): $p_m = 0$.

Dark Energy: $p_\Lambda = -\rho_\Lambda$.

Energy density

Radiation: $\rho_r \propto a^{-3}$.

Matter: $\rho_m \propto a^{-4}$.

Dark Energy: $\rho_\Lambda = \text{const.}$

the behaviour of $a(t)$ can only be modeled if we know $\Omega_i = \rho_i/\rho_{\text{crit}}$.

a sprinkle of thermodynamics

decoupling of a species

as we go back in time, the Universe was denser and warmer: early enough, all species were in *thermal equilibrium* and their distribution function $f^{(0)}$ was determined by statistics only.

a species is said to *decouple* when all its interactions proceed slower than the Universe's expansion, i.e. when $\Gamma < H = \dot{a}/a$.

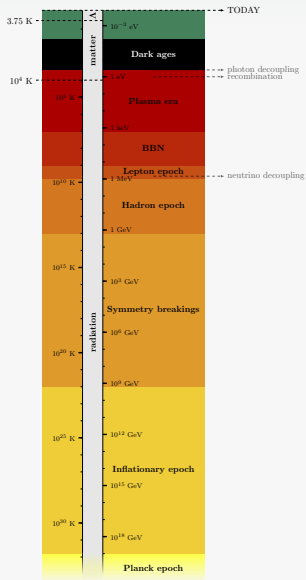
afterwards, $f = f^{(0)}$, but T behaves differently.

For photons:

$$f^{(0)} = \frac{1}{\exp(\nu/T) - 1},$$

with $T \propto a^{-1}$ before and after decoupling.

photon decoupling



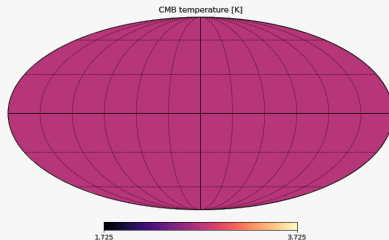
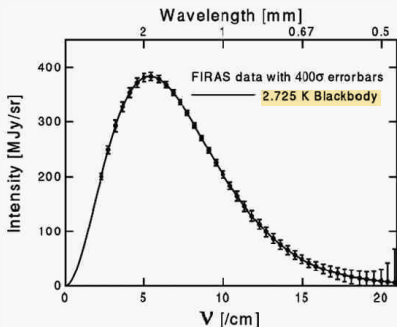
Recombination: as the Universe expanded, photons became less and less energetic, until they couldn't keep electrons and protons from combining into hydrogen atoms via $e^- + p \rightarrow H + \gamma$.

Photon decoupling: the drop of the number of free electrons, made it very unlikely for $e^- + \gamma \rightarrow e^- + \gamma$ scatterings to happen.

CMB: after decoupling, the photons travelled almost freely through space, characterized by a black-body spectrum.

observational evidence

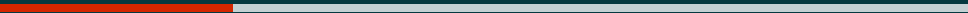
the CMB appears to be a perfect **black-body** at $\bar{T} = 2.725$ K.



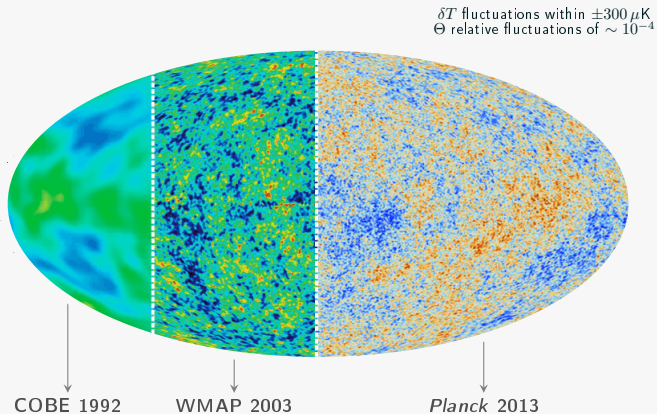
the temperature appears to be **isotropic** all over the sky.

**good agreement between theoretical predictions
for a FRW Universe and observations!**

beyond isotropy



a more refined picture



decomposition in spherical harmonics

The **spherical harmonics** $Y_{\ell m}(\hat{\mathbf{n}})$ are eigenfunctions of the Laplace operator on the sphere.

They can be used to write $\Theta(\hat{\mathbf{n}}) = \sum_{\ell=0}^{\infty} \sum_{m=-\ell}^{\ell} a_{\ell m} Y_{\ell m}(\hat{\mathbf{n}})$,

with **coefficients** $a_{\ell m} \equiv \int d^2n \Theta(\hat{\mathbf{n}}) Y_{\ell m}^*(\hat{\mathbf{n}})$.

If T is an isotropic random field, $\langle a_{\ell m} a_{\ell' m'}^* \rangle = \delta_{\ell \ell'} \delta_{m m'} C_{\ell}$.

$$C_{\ell} = \frac{1}{2\ell + 1} \sum_{m=-\ell}^{\ell} a_{\ell m} a_{\ell m}^*.$$

Y_{00}



Y_{10}



Y_{11}



Y_{20}



Y_{21}

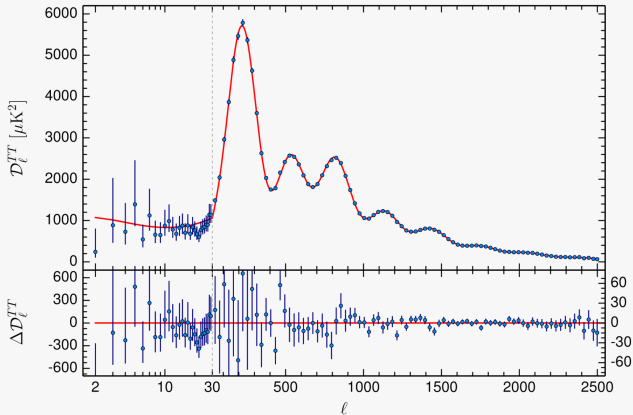


Y_{22}



Planck's angular power spectrum

$$\mathcal{D}_\ell \equiv \ell(\ell + 1)C_\ell/2\pi$$



a lot of **physical information** is encoded in the power spectrum.

understanding anisotropies

perturbed metric tensor

in order to work with δT or, equivalently, $\Theta \equiv \delta T/\bar{T}$, we need to abandon the isotropic and homogeneous description.

FRW metric: $ds^2 = -dt^2 + a^2 \delta_{ij} dx^i dx^j$

perturbed: $ds^2 = -(1 + 2\Phi)dt^2 + a^2 [(1 - 2\Psi)\delta_{ij} + h_{ij}] dx^i dx^j$.

cosmic fluids are also allowed to have perturbations: $\rho = \bar{\rho} + \delta\rho$.

geodesics in an expanding Universe

$$\frac{1}{p} \frac{dp}{dt} = -\frac{\dot{a}}{a} + \dot{\Psi} - \frac{1}{a} \sum_i \frac{\partial \Phi}{\partial x^i} \gamma^i - \frac{1}{2} \sum_{ij} \dot{h}_{ij} \gamma^i \gamma^j,$$

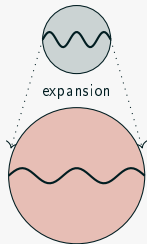
γ^i : unit vector in the direction of the photon momentum.

geodesics in an expanding Universe

$$\frac{1}{p} \frac{dp}{dt} = -\frac{\dot{a}}{a} + \dot{\Psi} - \frac{1}{a} \sum_i \frac{\partial \Phi}{\partial x^i} \gamma^i - \frac{1}{2} \sum_{ij} \dot{h}_{ij} \gamma^i \gamma^j,$$

γ^i : unit vector in the direction of the photon momentum.

cosmological redshift: wavelengths stretch as $\lambda \propto a$ and the photons' energy drops: $p \propto a^{-1}$.



geodesics in an expanding Universe

$$\frac{1}{p} \frac{dp}{dt} = -\frac{\dot{a}}{a} + \dot{\Psi} - \frac{1}{a} \sum_i \frac{\partial \Phi}{\partial x^i} \gamma^i - \frac{1}{2} \sum_{ij} \dot{h}_{ij} \gamma^i \gamma^j,$$

γ^i : unit vector in the direction of the photon momentum.

cosmological redshift: wavelengths stretch as $\lambda \propto a$ and the photons' energy drops: $p \propto a^{-1}$.

local scale factor: actually, $p \propto \tilde{a}^{-1}$, where

$$ds^2 = a^2(t)(1 - 2\Psi)d\mathbf{x}^2 \equiv \tilde{a}^2(t, \mathbf{x})d\mathbf{x}^2,$$

geodesics in an expanding Universe

$$\frac{1}{p} \frac{dp}{dt} = -\frac{\dot{a}}{a} + \dot{\Psi} - \frac{1}{a} \sum_i \frac{\partial \Phi}{\partial x^i} \gamma^i - \frac{1}{2} \sum_{ij} \dot{h}_{ij} \gamma^i \gamma^j,$$

γ^i : unit vector in the direction of the photon momentum.

cosmological redshift: wavelengths stretch as $\lambda \propto a$ and the photons' energy drops: $p \propto a^{-1}$.

local scale factor: actually, $p \propto \tilde{a}^{-1}$, where

$$ds^2 = a^2(t)(1 - 2\Psi)d\mathbf{x}^2 \equiv \tilde{a}^2(t, \mathbf{x})d\mathbf{x}^2,$$

gravitational shift: photons **gain** (**lose**) energy **falling into** (**climbing out of**) a potential well.

geodesics in an expanding Universe

$$\frac{1}{p} \frac{dp}{dt} = -\frac{\dot{a}}{a} + \dot{\Psi} - \frac{1}{a} \sum_i \frac{\partial \Phi}{\partial x^i} \gamma^i - \frac{1}{2} \sum_{ij} \dot{h}_{ij} \gamma^i \gamma^j,$$

γ^i : unit vector in the direction of the photon momentum.

cosmological redshift: wavelengths stretch as $\lambda \propto a$ and the photons' energy drops: $p \propto a^{-1}$.

local scale factor: actually, $p \propto \tilde{a}^{-1}$, where

$$ds^2 = a^2(t)(1 - 2\Psi)d\mathbf{x}^2 \equiv \tilde{a}^2(t, \mathbf{x})d\mathbf{x}^2,$$

gravitational shift: photons **gain** (loose) energy **falling into** (climbing out of) a potential well.

gravitational shift: additional gravitational red/blueshift due to tensor perturbations.

line of sight integration

integrating between the time of decoupling and today (*only scalar!*):

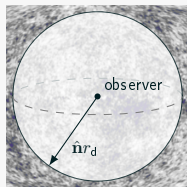
$$\Theta(\hat{\mathbf{n}}) = \frac{\delta_{\gamma}(t_d, \hat{\mathbf{n}}r_d)}{4} + \Phi(t_d, \hat{\mathbf{n}}r_d) - \Phi(t_0, \hat{\mathbf{n}}r_0) + \int_{t_d}^{t_0} dt (\dot{\Phi} + \dot{\Psi})(t, \hat{\mathbf{n}}r).$$

line of sight integration

integrating between the time of decoupling and today (*only scalar!*):

$$\Theta(\hat{\mathbf{n}}) = \frac{\delta_\gamma(t_d, \hat{\mathbf{n}}r_d)}{4} + \Phi(t_d, \hat{\mathbf{n}}r_d) - \Phi(t_0, \hat{\mathbf{n}}r_0) + \int_{t_d}^{t_0} dt (\dot{\Phi} + \dot{\Psi})(t, \hat{\mathbf{n}}r).$$

initial conditions: relative density fluctuations $\delta_\gamma(t_d, \hat{\mathbf{n}}r_d) \equiv \delta\rho_\gamma(t_d, \hat{\mathbf{n}}r_d)/\bar{\rho}_\gamma(t_d)$ at the time of photon decoupling.



line of sight integration

integrating between the time of decoupling and today (*only scalar!*):

$$\Theta(\hat{\mathbf{n}}) = \frac{\delta_\gamma(t_d, \hat{\mathbf{n}}r_d)}{4} + \Phi(t_d, \hat{\mathbf{n}}r_d) - \Phi(t_0, \hat{\mathbf{n}}r_0) + \int_{t_d}^{t_0} dt (\dot{\Phi} + \dot{\Psi})(t, \hat{\mathbf{n}}r).$$

initial conditions: relative density fluctuations $\delta_\gamma(t_d, \hat{\mathbf{n}}r_d) \equiv \delta\rho_\gamma(t_d, \hat{\mathbf{n}}r_d)/\bar{\rho}_\gamma(t_d)$ at the time of photon decoupling.

gravitational red/blueshift: depending on the values of Φ when the photons decoupled and reached us, they gained/lost energy.

line of sight integration

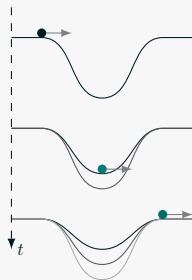
integrating between the time of decoupling and today (*only scalar!*):

$$\Theta(\hat{\mathbf{n}}) = \frac{\delta_\gamma(t_d, \hat{\mathbf{n}}r_d)}{4} + \Phi(t_d, \hat{\mathbf{n}}r_d) - \Phi(t_0, \hat{\mathbf{n}}r_0) + \int_{t_d}^{t_0} dt (\dot{\Phi} + \dot{\Psi})(t, \hat{\mathbf{n}}r).$$

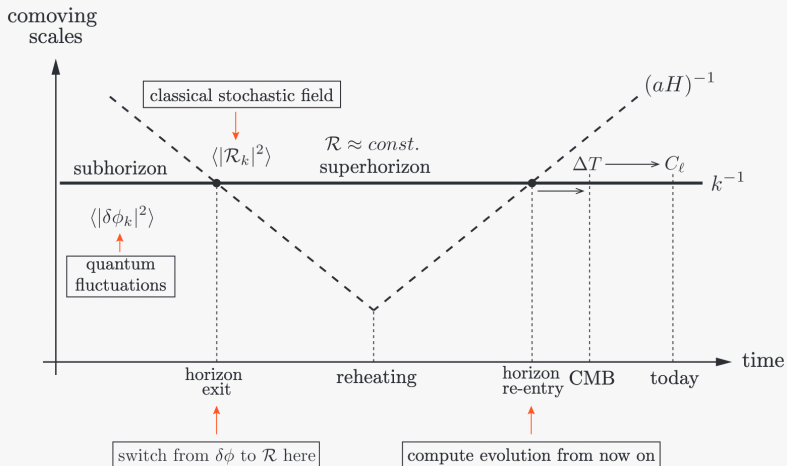
initial conditions: relative density fluctuations $\delta_\gamma(t_d, \hat{\mathbf{n}}r_d) \equiv \delta\rho_\gamma(t_d, \hat{\mathbf{n}}r_d)/\bar{\rho}_\gamma(t_d)$ at the time of photon decoupling.

gravitational red/blueshift: depending on the values of Φ when the photons decoupled and reached us, they gained/lost energy.

ISW effect: photons can gain more energy than they lose (or viceversa) if Φ depends on time.



initial conditions from inflation



a window on the Early Universe

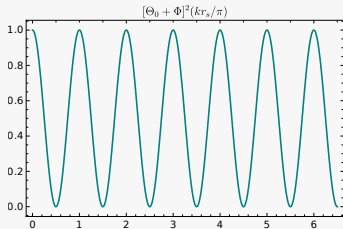
$\Theta(\hat{\mathbf{n}})$ depends on the physics at decoupling via the initial conditions $[\delta_\gamma/4 + \Phi](t_d, \hat{\mathbf{n}}r_d) \equiv [\delta_\gamma/4 + \Phi]_d$, which can be related to the **primordial** Φ_{in} in Fourier space:

$$\left[\frac{\delta_\gamma}{4} + \Phi \right]_d = \frac{3\Phi_{\text{in}}}{10} \left[3R_b \mathcal{T}(k) - \frac{\mathcal{S}(k) \cos[kr_s + \Delta(k)]}{(1 + R_b)^{1/4}} \right],$$

a window on the Early Universe

$\Theta(\hat{\mathbf{n}})$ depends on the physics at decoupling via the initial conditions $[\delta_\gamma/4 + \Phi](t_d, \hat{\mathbf{n}}r_d) \equiv [\delta_\gamma/4 + \Phi]_d$, which can be related to the **primordial** Φ_{in} in Fourier space:

$$\left[\frac{\delta_\gamma}{4} + \Phi \right]_d = \frac{3\Phi_{\text{in}}}{10} \left[3R_b \mathcal{T}(k) - \frac{\mathcal{S}(k) \cos[kr_s + \Delta(k)]}{(1 + R_b)^{1/4}} \right],$$

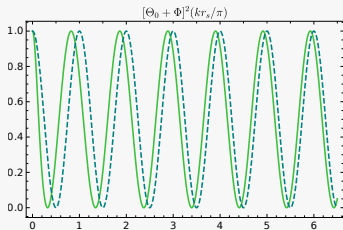


$$\begin{aligned} R_b &= 0, \\ \mathcal{S}(k) &= 0, \\ \Delta(k) &= 0. \end{aligned}$$

a window on the Early Universe

$\Theta(\hat{\mathbf{n}})$ depends on the physics at decoupling via the initial conditions $[\delta_\gamma/4 + \Phi](t_d, \hat{\mathbf{n}}r_d) \equiv [\delta_\gamma/4 + \Phi]_d$, which can be related to the **primordial** Φ_{in} in Fourier space:

$$\left[\frac{\delta_\gamma}{4} + \Phi \right]_d = \frac{3\Phi_{\text{in}}}{10} \left[3R_b \mathcal{T}(k) - \frac{\mathcal{S}(k) \cos[kr_s + \Delta(k)]}{(1 + R_b)^{1/4}} \right],$$

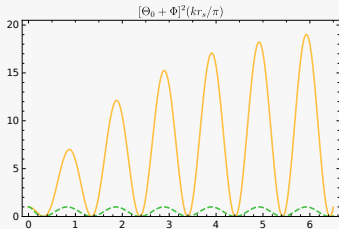


$$R_b = 0,$$
$$\mathcal{S}(k) = 0,$$

a window on the Early Universe

$\Theta(\hat{\mathbf{n}})$ depends on the physics at decoupling via the initial conditions $[\delta_\gamma/4 + \Phi](t_d, \hat{\mathbf{n}}r_d) \equiv [\delta_\gamma/4 + \Phi]_d$, which can be related to the **primordial** Φ_{in} in Fourier space:

$$\left[\frac{\delta_\gamma}{4} + \Phi \right]_d = \frac{3\Phi_{\text{in}}}{10} \left[3R_b \mathcal{T}(k) - \frac{\mathcal{S}(k) \cos[kr_s + \Delta(k)]}{(1 + R_b)^{1/4}} \right],$$

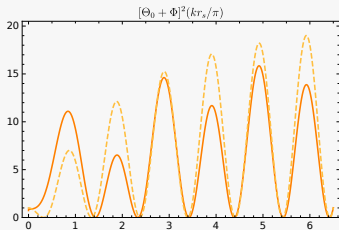


$$R_b = 0,$$

a window on the Early Universe

$\Theta(\hat{\mathbf{n}})$ depends on the physics at decoupling via the initial conditions $[\delta_\gamma/4 + \Phi](t_d, \hat{\mathbf{n}}r_d) \equiv [\delta_\gamma/4 + \Phi]_d$, which can be related to the **primordial** Φ_{in} in Fourier space:

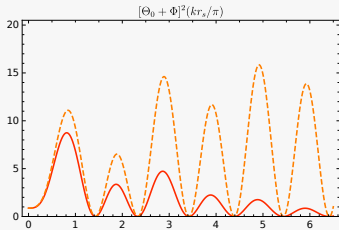
$$\left[\frac{\delta_\gamma}{4} + \Phi \right]_d = \frac{3\Phi_{\text{in}}}{10} \left[3R_b \mathcal{T}(k) - \frac{\mathcal{S}(k) \cos[kr_s + \Delta(k)]}{(1 + R_b)^{1/4}} \right],$$



a window on the Early Universe

$\Theta(\hat{\mathbf{n}})$ depends on the physics at decoupling via the initial conditions $[\delta_\gamma/4 + \Phi](t_d, \hat{\mathbf{n}}r_d) \equiv [\delta_\gamma/4 + \Phi]_d$, which can be related to the **primordial** Φ_{in} in Fourier space:

$$\left[\frac{\delta_\gamma}{4} + \Phi \right]_d = \frac{3\Phi_{\text{in}}}{10} \left[3R_b \mathcal{T}(k) - \frac{\mathcal{S}(k) \cos[kr_s + \Delta(k)]}{(1 + R_b)^{1/4}} \right],$$

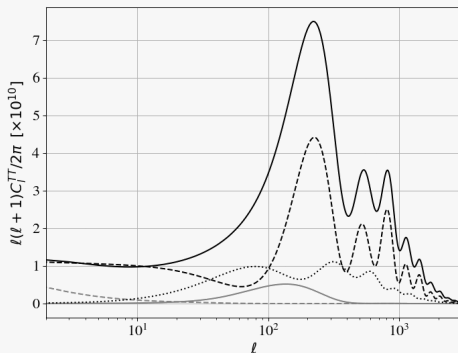


different photons decouple at slightly different times, leading to a suppression on small scales.

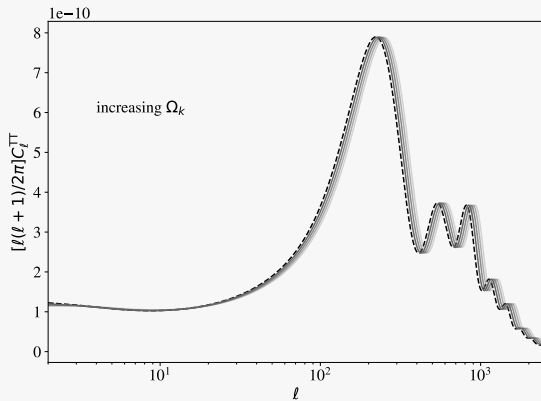
getting to the C_ℓ

$$\Theta(\hat{\mathbf{n}}) = \frac{\delta_\gamma(t_d, \hat{\mathbf{n}}r_d)}{4} + \Phi(t_d, \hat{\mathbf{n}}r_d) - \Phi(t_0, \hat{\mathbf{n}}r_0) + \int_{t_d}^{t_0} dt (\dot{\Phi} + \dot{\Psi})(t, \hat{\mathbf{n}}r).$$

dashed black line gray lines



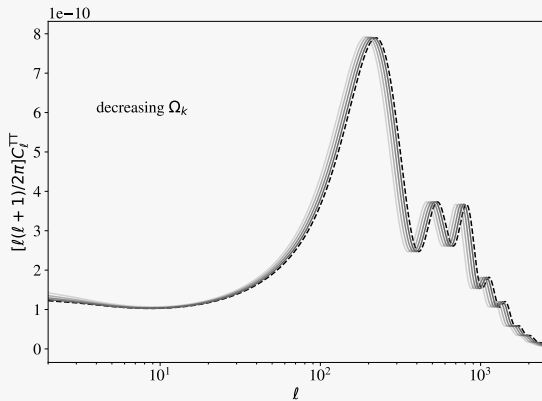
extracting cosmology from the C_ℓ



curvature k



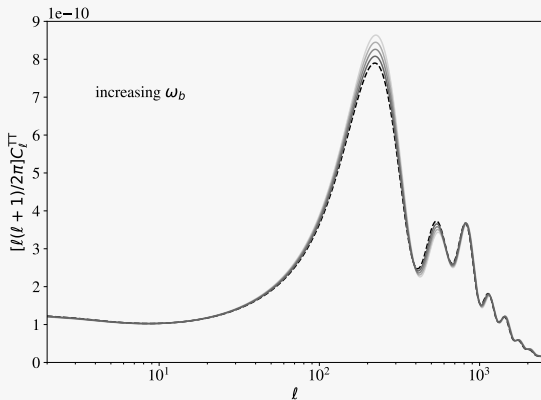
extracting cosmology from the C_ℓ



curvature k



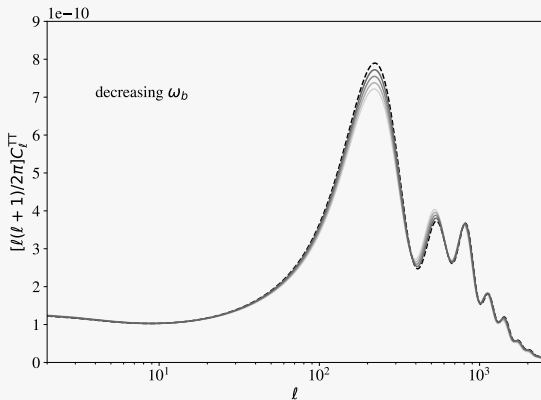
extracting cosmology from the C_ℓ



baryons

baryons shift vertically the oscillations at decoupling: when taking the square, even/odd peaks are enhanced/suppressed.

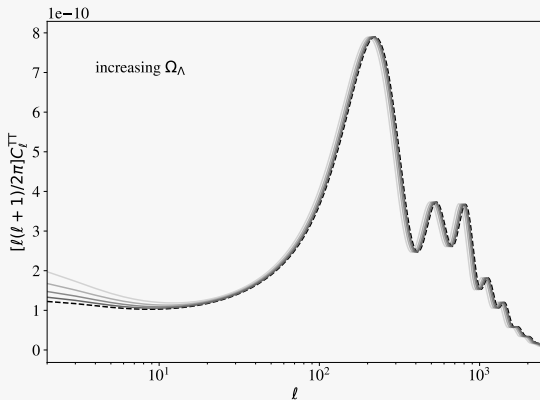
extracting cosmology from the C_ℓ



baryons

baryons shift vertically the oscillations at decoupling: when taking the square, even/odd peaks are enhanced/suppressed.

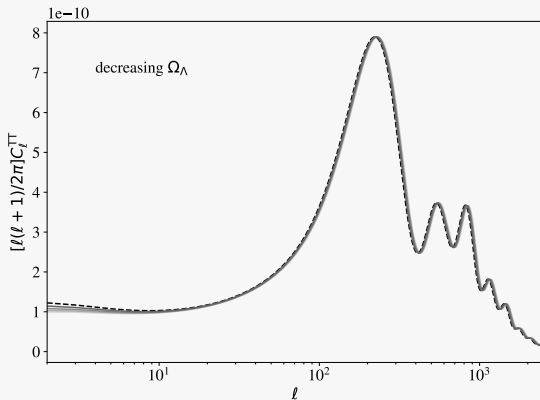
extracting cosmology from the C_ℓ



Dark Energy

Dark Energy cannot affect the physics at decoupling, but affects the ISW low- l plateau.

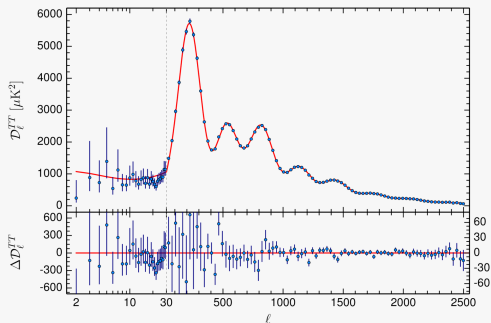
extracting cosmology from the C_ℓ



Dark Energy

Dark Energy cannot affect the physics at decoupling, but affects the ISW low- l plateau.

best-fit *Planck* cosmological parameters

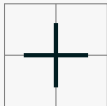


Parameter	<i>Planck</i> alone
$\Omega_b h^2$	0.02237 ± 0.00015
$\Omega_c h^2$	0.1200 ± 0.0012
$100\theta_{MC}$	1.04092 ± 0.00031
τ	0.0544 ± 0.0073
$\ln(10^{10} A_s)$	3.044 ± 0.014
n_s	0.9649 ± 0.0042
H_0	67.36 ± 0.54
Ω_K	-0.0096 ± 0.0061
Σm_ν [eV]	< 0.241
N_{eff}	$2.89^{+0.36}_{-0.38}$
$r_{0.002}$	< 0.101

polarization

describing polarization

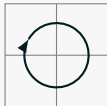
unpolarized



linear



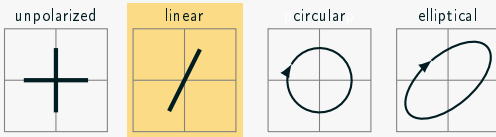
circular



elliptical

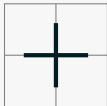


describing polarization



describing polarization

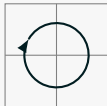
unpolarized



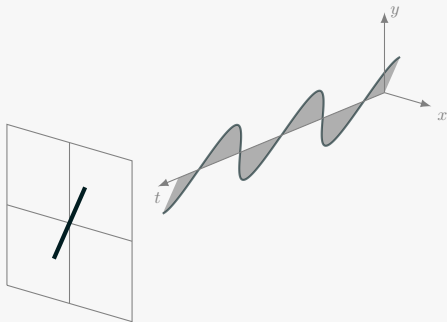
linear



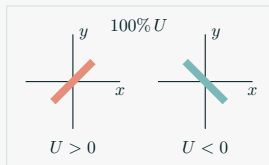
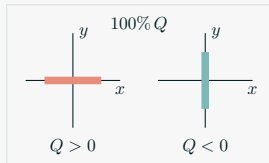
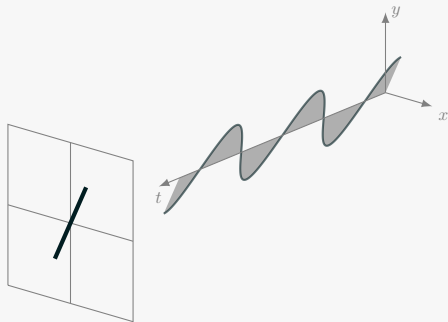
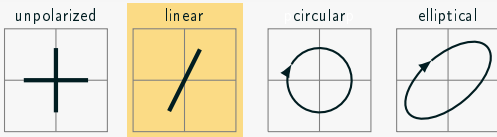
circular



elliptical



describing polarization



describing polarization: E - and B -modes

issue: (Q, U) are coordinate dependent!

for instance, rotating the coordinate system of 45° clockwise sends
 $Q \rightarrow -U$ and $U \rightarrow Q$.

describing polarization: E - and B -modes

issue: (Q, U) are coordinate dependent!

for instance, rotating the coordinate system of 45° clockwise sends
 $Q \rightarrow -U$ and $U \rightarrow Q$.

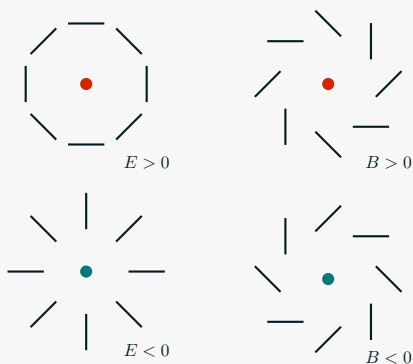
(E, B) -modes are coordinate-independent *non-local* combinations of (Q, U) .

describing polarization: E - and B -modes

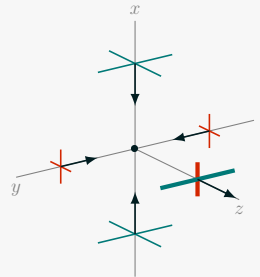
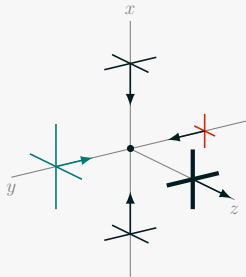
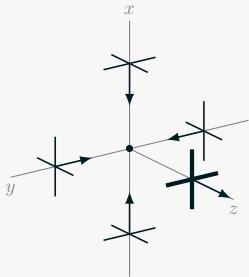
issue: (Q, U) are coordinate dependent!

for instance, rotating the coordinate system of 45° clockwise sends
 $Q \rightarrow -U$ and $U \rightarrow Q$.

(E, B) -modes are coordinate-independent *non-local* combinations of (Q, U) .

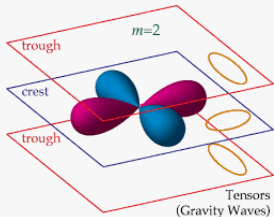
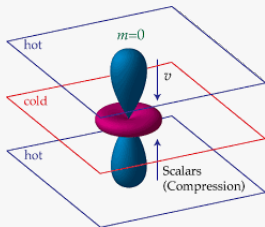


polarization from last-scattering



polarization can only be produced if the temperature distribution
around the electron at decoupling has a quadrupole patten.

quadrupole from scalar vs tensor modes



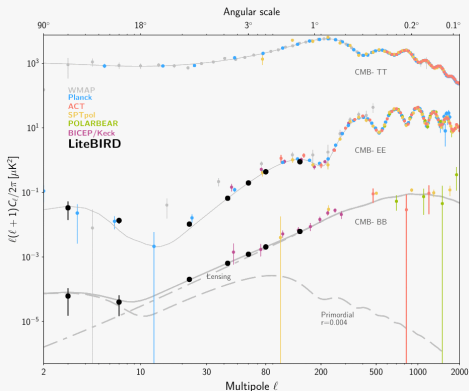
both scalar and tensor modes can have a quadrupole pattern,
however, **scalar modes can only generate E -modes.**

searching B -modes from inflation

Expectation: inflation-sourced perturbations leave traces on the CMB polarization.

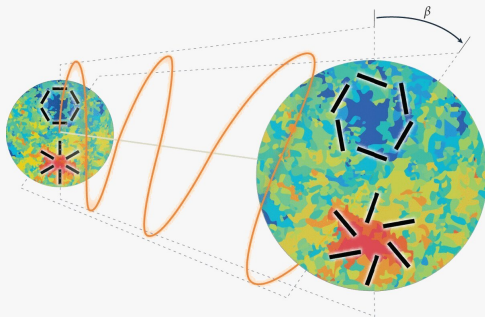
Large scale B -modes can probe inflation.

Unprecedented sensitivity requirements!



a side effect: measuring cosmic birefringence

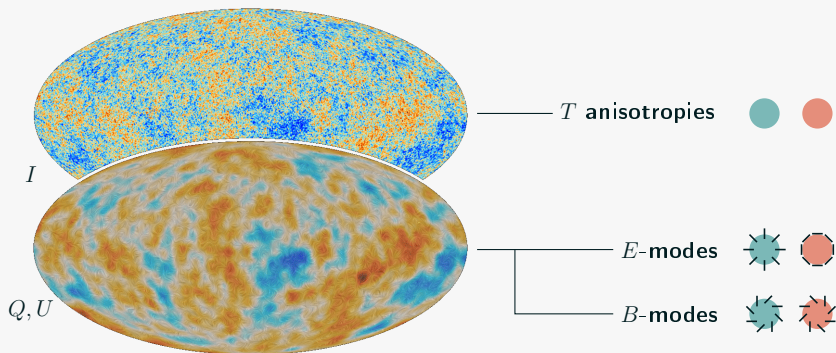
CMB might also carry information about parity-violating new physics: **cosmic birefringence**.
(time-dependent parity-violating pseudoscalar field)



mixing of E and B modes:
$$\begin{cases} a_{\ell m, \text{obs}}^E = a_{\ell m}^E \cos 2\beta - a_{\ell m}^B \sin 2\beta, \\ a_{\ell m, \text{obs}}^B = a_{\ell m}^E \sin 2\beta + a_{\ell m}^B \cos 2\beta. \end{cases}$$

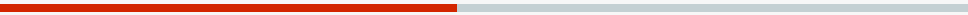
to sum up

CMB anisotropies



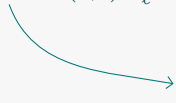
ongoing efforts to refine the detection of CMB polarization:
potential probe of inflation and cosmic birefringence.

backup



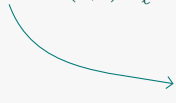
trying to constrain β

$$\left\{ \begin{array}{l} C_{l,\text{obs}}^{TT} = C_l^{TT}, \\ C_{l,\text{obs}}^{EE} = \cos^2(2\beta)C_l^{EE} + \sin^2(2\beta)C_l^{BB} - \sin(4\beta)C_l^{EB}, \\ C_{l,\text{obs}}^{BB} = \cos^2(2\beta)C_l^{BB} + \sin^2(2\beta)C_l^{EE} + \sin(4\beta)C_l^{EB}, \\ C_{l,\text{obs}}^{TE} = \cos(2\beta)C_l^{TE} - \sin(2\beta)C_l^{TB}, \\ C_{l,\text{obs}}^{EB} = \sin(4\beta)(C_l^{EE} - C_l^{BB})/2 + \cos(4\beta)C_l^{EB}, \\ C_{l,\text{obs}}^{TB} = \sin(2\beta)C_l^{TE} + \cos(2\beta)C_l^{TB}. \end{array} \right.$$


$$C_{l,\text{obs}}^{EB} = \tan(4\beta)(C_{l,\text{obs}}^{EE} - C_{l,\text{obs}}^{BB})/2.$$

trying to constrain β

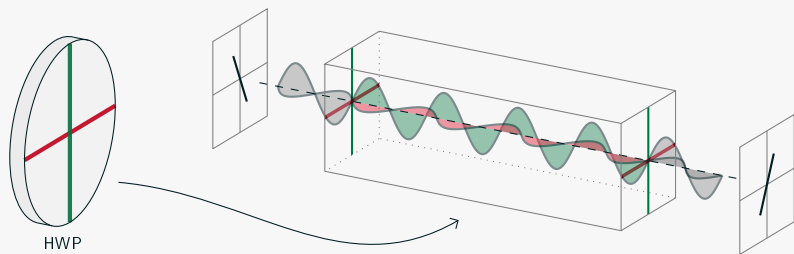
$$\begin{cases} C_{\ell,\text{obs}}^{TT} = C_{\ell}^{TT}, \\ C_{\ell,\text{obs}}^{EE} = \cos^2(2\beta)C_{\ell}^{EE} + \sin^2(2\beta)C_{\ell}^{BB} - \sin(4\beta)C_{\ell}^{EB}, \\ C_{\ell,\text{obs}}^{BB} = \cos^2(2\beta)C_{\ell}^{BB} + \sin^2(2\beta)C_{\ell}^{EE} + \sin(4\beta)C_{\ell}^{EB}, \\ C_{\ell,\text{obs}}^{TE} = \cos(2\beta)C_{\ell}^{TE} - \sin(2\beta)C_{\ell}^{TB}, \\ C_{\ell,\text{obs}}^{EB} = \sin(4\beta)(C_{\ell}^{EE} - C_{\ell}^{BB})/2 + \cos(4\beta)C_{\ell}^{EB}, \\ C_{\ell,\text{obs}}^{TB} = \sin(2\beta)C_{\ell}^{TE} + \cos(2\beta)C_{\ell}^{TB}. \end{cases}$$


$$C_{\ell,\text{obs}}^{EB} = \tan(4\beta)(C_{\ell,\text{obs}}^{EE} - C_{\ell,\text{obs}}^{BB})/2.$$

$$\beta = 0.35 \pm 0.14 \text{ (68\%CL)}$$

To extract this kind of information from CMB
systematics have to be kept under control.

the HWP: reducing systematics



A **rotating** half-wave plate (HWP) as first optical element:

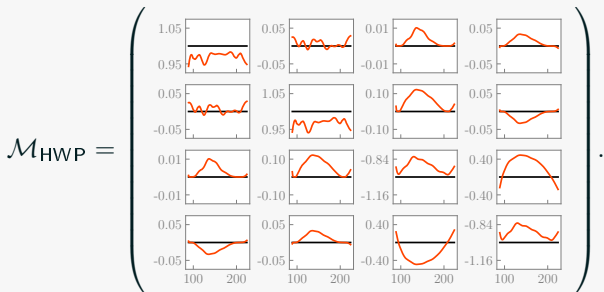
modulates the signal to $4f_{\text{HWP}}$, allowing to “escape” $1/f$ noise;

makes possible for a single detector to measure polarization, reducing pair-differencing systematics.

the HWP: inducing systematics

Mueller calculus: radiation described as $S = (I, Q, U, V)$, effect of polarization-altering devices parametrized by \mathcal{M} : so that $S' = \mathcal{M} \cdot S$.

For an ideal HWP, $\mathcal{M}_{\text{ideal}} = \text{diag}(1, 1, -1, -1)$, but let's look at a realistic case:



how does this affect the observed maps?

steps we took in that direction

- work on a **simulation pipeline** for a LiteBIRD-like mission;
- simulate observed maps in presence of non-ideal HWP;
- derive **analytical formulae** to interpret the output.

PREPARED FOR SUBMISSION TO JCAP

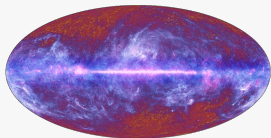
Impact of half-wave plate systematics on the measurement of **cosmic birefringence** from CMB polarization

Marta Monelli,^a Eiichiro Komatsu,^{a,b} Alexandre Adler,^c Matteo Billi,^{d,e,f} Paolo Campeti,^{a,g} Nadia Dachlythra,^c Adriaan Duivenvoorden,^h Jon Gudmundsson,^c and Martin Reinecke.^a

simulations

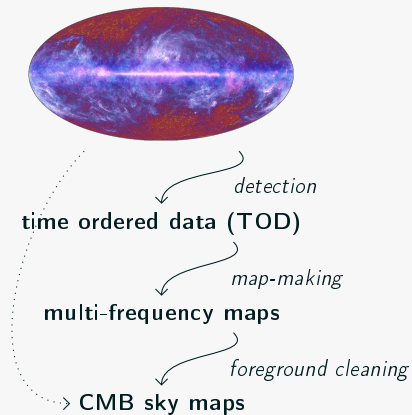


what do we simulate

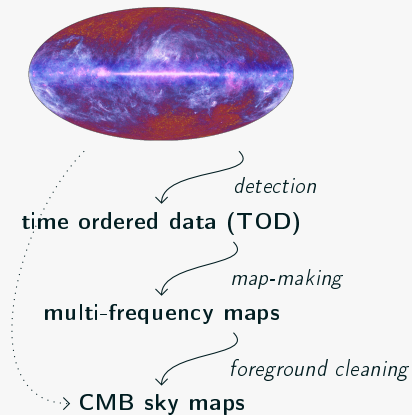


→ CMB sky maps

what do we simulate

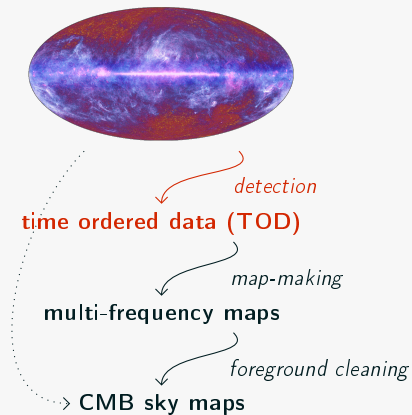


what do we simulate



TOD: collection of the signal detected by *each of the (4508) detectors* during the *whole (3-year) mission*.

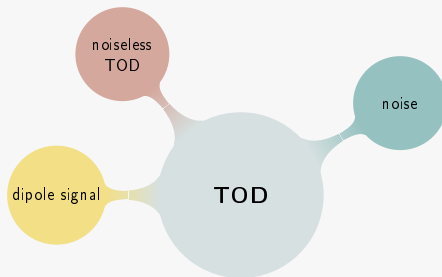
what do we simulate



TOD: collection of the signal detected by *each of the (4508) detectors* during the *whole (3-year) mission*.

Simulating TOD is crucial in the planning of any CMB experiment: helps studying potential systematic effects.

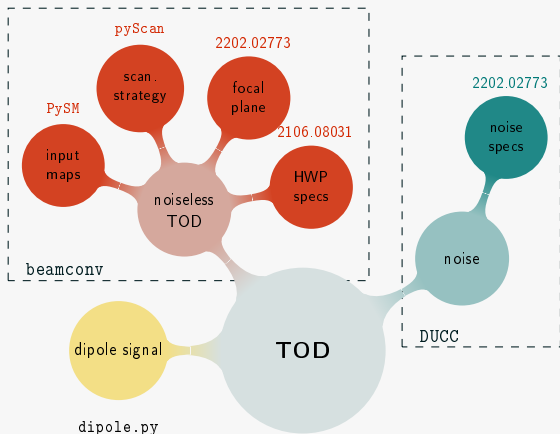
sketch of the pipeline



sketch of the pipeline

beamconv: convolution code simulating TOD for CMB experiments with realistic polarized **beams**, scanning strategies and **HWP**.

DUCC: collection of basic programming tools for numerical computation: `fft`, `sht`, `healpix`, `totalconvolve`...



working assumptions

To focus on the impact of **HWP non-idealities**, we consider a simplified problem:

no noise,

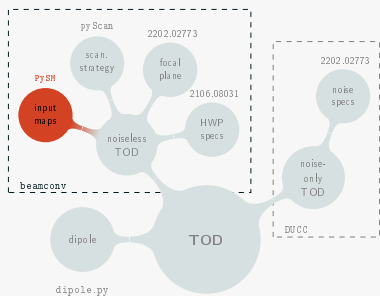
single frequency,

CMB-only,

simple beams,

HWP aligned to the detector line of sight.

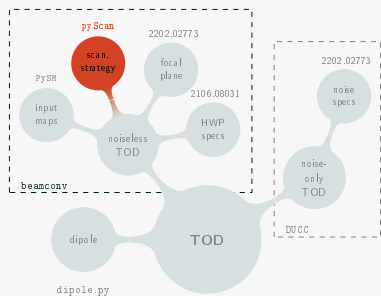
input maps



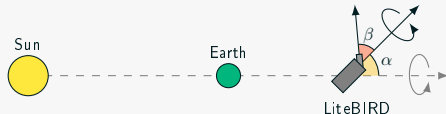
The pipeline can be fed with arbitrary input maps: **CMB**, **foregrounds**, or both.

In the paper: I , Q and U input maps with $n_{\text{side}} = 512$ from best-fit 2018 Planck power spectra;

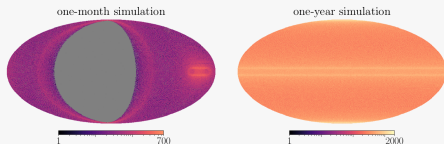
scanning strategy



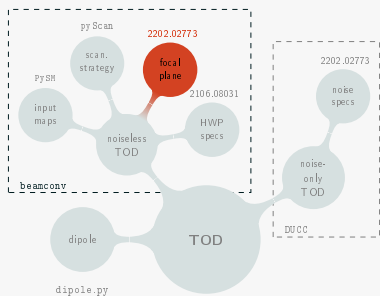
The pipeline can read or calculate pointings. We implemented some functionalities of pyScan in beamconv to deal with satellite missions.



In the paper: 1 year of LiteBIRD-like scanning strategy.



focal plane specifics



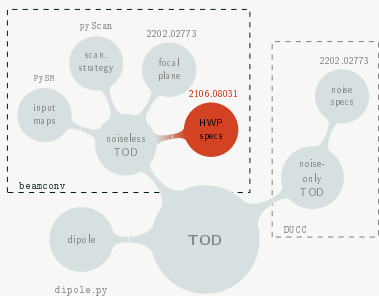
The pipeline can read from the Instrument Model Database (IMO):

```
{'name': 'M02_030_QA_140T',
  'wafer': 'M02',
  'pixel': 30,
  'pixtype': 'MP1',
  [...],
  'pol': 'T',
  'orient': 'Q',
  'quat': [1, 0, 0, 0]}
```

In the paper: 160 dets from M1-140.

specs.	values
f_{samp}	19 Hz
HWP rpm	39
FWHM	30.8 arcmin
offset quats.	[...]

HWP specifics



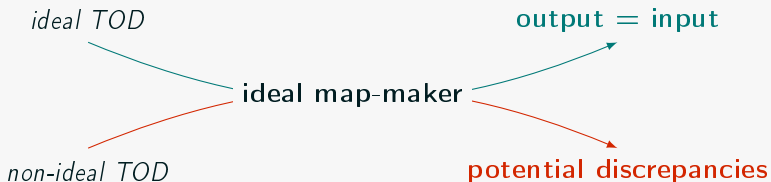
In the paper: HWP is assumed to be ideal in the **first** simulation run (ideal TOD) and realistic in the **second** (non-ideal TOD).

Realistic HWP Mueller matrix elements as shown previously:

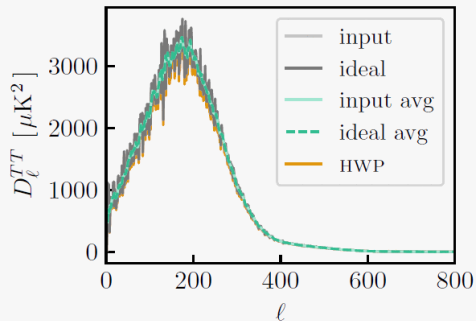
$$\mathcal{M}_{\text{HWP}} = \begin{pmatrix} \begin{matrix} 1.05 & 0.05 & 0.01 & 0.05 \\ 0.95 & -0.05 & -0.01 & -0.05 \end{matrix} \\ \begin{matrix} 0.05 & 1.05 & 0.10 & 0.05 \\ -0.05 & 0.95 & -0.10 & -0.05 \end{matrix} \\ \begin{matrix} 0.01 & 0.10 & -0.84 & 0.40 \\ -0.01 & -0.10 & -1.16 & -0.40 \end{matrix} \\ \begin{matrix} 0.05 & 0.05 & -0.84 & 0.40 \\ -0.05 & -0.05 & -0.40 & -1.16 \end{matrix} \end{pmatrix}.$$

what about maps?

Both ideal and non-ideal TOD processed by **ideal** bin-averaging map-maker.



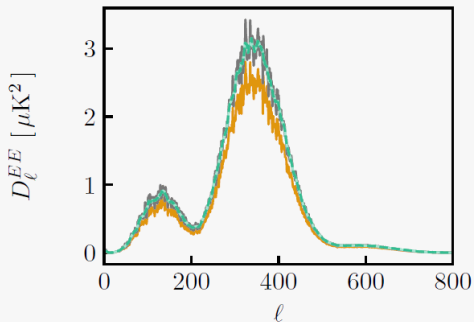
ideal vs non-ideal output spectra (1)



(beam transfer function not deconvolved)

TT leaked a bit

ideal vs non-ideal output spectra (1)

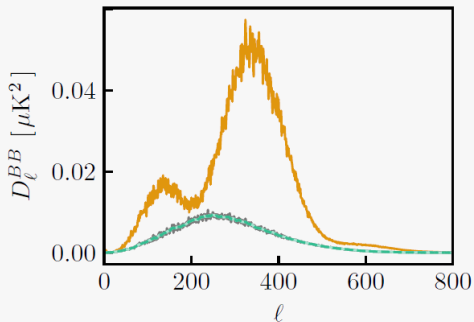


(beam transfer function not deconvolved)

TT leaked a bit

EE leaked a lot!

ideal vs non-ideal output spectra (1)



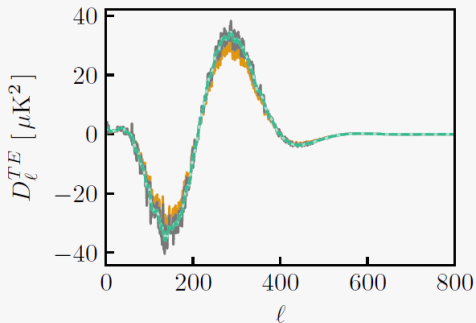
(beam transfer function not deconvolved)

TT leaked a bit

EE leaked a lot!

BB larger (*EE* shape!)

ideal vs non-ideal output spectra (1)



(beam transfer function not deconvolved)

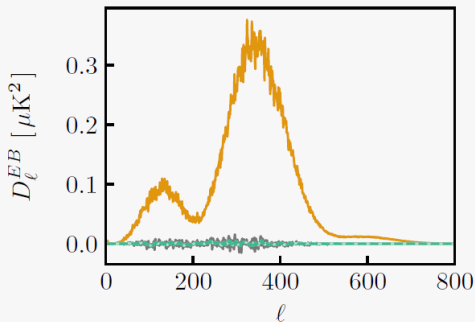
TT leaked a bit

EE leaked a lot!

BB larger (*EE* shape!)

TE leaked a bit

ideal vs non-ideal output spectra (1)



(beam transfer function not deconvolved)

TT leaked a bit

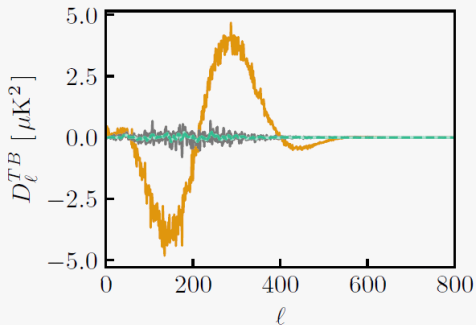
EE leaked a lot!

BB larger (*EE* shape!)

TE leaked a bit

EB non-zero!

ideal vs non-ideal output spectra (1)



(beam transfer function not deconvolved)

TT leaked a bit

EE leaked a lot!

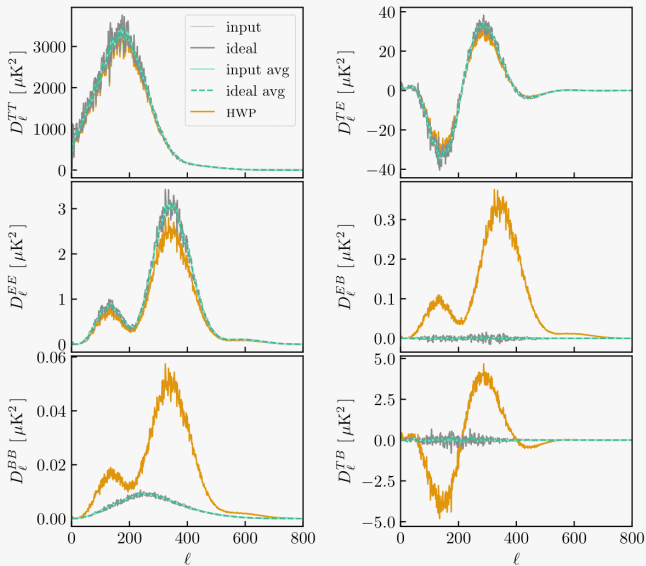
BB larger (*EE* shape!)

TE leaked a bit

EB non-zero!

TB non-zero!

ideal vs non-ideal output spectra (2)



how can we understand this?

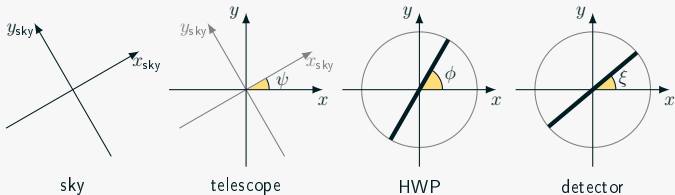
modeling the TOD

How beamconv computes the TOD:

$$d_t = \sum_{s\ell m} \left[B_{\ell s}^I a_{\ell m}^I + \frac{1}{2} (-2B_{\ell s}^P a_{\ell m}^P + 2B_{\ell s}^P - 2a_{\ell m}^P) + B_{\ell s}^V a_{\ell m}^V \right] \sqrt{\frac{4\pi}{2\ell+1}} e^{-is\psi_t} {}_s Y_{\ell m}(\theta_t, \phi_t),$$

beam coefficients (or combinations of them if HWP non-ideal).

In the paper: $d = (1 \ 0 \ 0) \cdot \mathcal{M}_{\det} \mathcal{R}_{\xi-\phi} \mathcal{M}_{\text{HWP}} \mathcal{R}_{\phi+\psi} \cdot \mathbf{S}$.



modeling the observed maps

(minimal) TOD: signal detected by 4 detectors.

map-maker: bin-averaging assuming ideal HWP.

estimated output maps: linear combination of $\{I, Q, U\}_{\text{in}}$.

$$\begin{pmatrix} d^{(0)} \\ d^{(90)} \\ d^{(45)} \\ d^{(135)} \end{pmatrix} = \begin{pmatrix} (1 \ 0 \ 0) \cdot \mathcal{M}_{\text{det}} \mathcal{R}_{0-\phi} \mathcal{M}_{\text{HWP}} \mathcal{R}_{\phi+\psi} \\ (1 \ 0 \ 0) \cdot \mathcal{M}_{\text{det}} \mathcal{R}_{90-\phi} \mathcal{M}_{\text{HWP}} \mathcal{R}_{\phi+\psi} \\ (1 \ 0 \ 0) \cdot \mathcal{M}_{\text{det}} \mathcal{R}_{45-\phi} \mathcal{M}_{\text{HWP}} \mathcal{R}_{\phi+\psi} \\ (1 \ 0 \ 0) \cdot \mathcal{M}_{\text{det}} \mathcal{R}_{135-\phi} \mathcal{M}_{\text{HWP}} \mathcal{R}_{\phi+\psi} \end{pmatrix} \cdot \begin{pmatrix} I_{\text{in}} \\ Q_{\text{in}} \\ U_{\text{in}} \end{pmatrix}$$

Being *ideal*, map-making amounts to apply $(\hat{A}^T \hat{A})^{-1} \hat{A}^T$ to the TOD:

$$\hat{S} = (\hat{A}^T \hat{A})^{-1} \hat{A}^T A \cdot S.$$

estimated output maps

$$\begin{aligned}\hat{I} &= m_{ii}I_{\text{in}} + (m_{iq}Q_{\text{in}} + m_{iu}U_{\text{in}}) \cos(2\alpha) + (m_{iq}U_{\text{in}} - m_{iu}Q_{\text{in}}) \sin(2\alpha), \\ \hat{Q} &= \frac{1}{2} \left\{ (m_{qq} - m_{uu})Q_{\text{in}} + (m_{qu} + m_{uq})U_{\text{in}} + 2m_{qi}I_{\text{in}} \cos(2\alpha) + 2m_{ui}I_{\text{in}} \sin(2\alpha) \right. \\ &\quad + [(m_{qq} + m_{uu})Q_{\text{in}} + (m_{qu} - m_{uq})U_{\text{in}}] \cos(4\alpha) \\ &\quad \left. + [-(m_{qu} - m_{uq})Q_{\text{in}} + (m_{qq} + m_{uu})U_{\text{in}}] \sin(4\alpha) \right\}, \\ \hat{U} &= \frac{1}{2} \left\{ (m_{qq} - m_{uu})U_{\text{in}} - (m_{qu} + m_{uq})Q_{\text{in}} - 2m_{ui}I_{\text{in}} \cos(2\alpha) + 2m_{qi}I_{\text{in}} \sin(2\alpha) \right. \\ &\quad + [-(m_{qq} + m_{uu})U_{\text{in}} + (m_{qu} - m_{uq})Q_{\text{in}}] \cos(4\alpha) \\ &\quad \left. + [(m_{qu} - m_{uq})U_{\text{in}} + (m_{qq} + m_{uu})Q_{\text{in}}] \sin(4\alpha) \right\},\end{aligned}$$

where $\alpha = \phi + \psi$. For **good** coverage and **rapidly spinning** HWP:

$$\hat{\mathbf{S}} \simeq \begin{pmatrix} m_{ii}I_{\text{in}} \\ [(m_{qq} - m_{uu})Q_{\text{in}} + (m_{qu} + m_{uq})U_{\text{in}}]/2 \\ [-(m_{qu} + m_{uq})Q_{\text{in}} + (m_{qq} - m_{uu})U_{\text{in}}]/2 \end{pmatrix}.$$

equations for the \widehat{C}_ℓ s

Expanding \widehat{S} in spherical harmonics:

$$\widehat{C}_\ell^{TT} \simeq m_{ii}^2 C_{\ell,\text{in}}^{TT},$$

$$\widehat{C}_\ell^{EE} \simeq \frac{(m_{qq} - m_{uu})^2}{4} C_{\ell,\text{in}}^{EE} + \frac{(m_{qu} + m_{uq})^2}{4} C_{\ell,\text{in}}^{BB} + \frac{(m_{qq} - m_{uu})(m_{qu} + m_{uq})}{2} C_{\ell,\text{in}}^{EB},$$

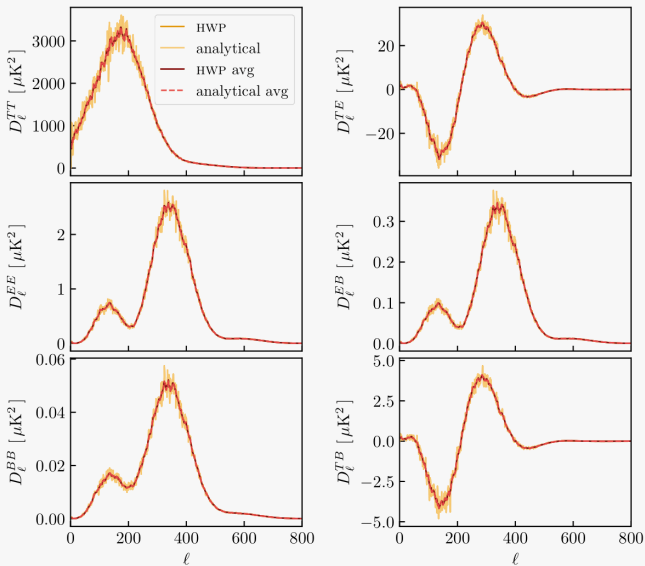
$$\widehat{C}_\ell^{BB} \simeq \frac{(m_{qq} - m_{uu})^2}{4} C_{\ell,\text{in}}^{BB} + \frac{(m_{qu} + m_{uq})^2}{4} C_{\ell,\text{in}}^{EE} - \frac{(m_{qq} - m_{uu})(m_{qu} + m_{uq})}{2} C_{\ell,\text{in}}^{EB},$$

$$\widehat{C}_\ell^{TE} \simeq \frac{m_{ii}(m_{qq} - m_{uu})}{2} C_{\ell,\text{in}}^{TE} + \frac{m_{ii}(m_{qu} + m_{uq})}{2} C_{\ell,\text{in}}^{TB},$$

$$\widehat{C}_\ell^{EB} \simeq \frac{(m_{qq} - m_{uu})^2 - (m_{qu} + m_{uq})^2}{4} C_{\ell,\text{in}}^{EB} - \frac{(m_{qq} - m_{uu})(m_{qu} + m_{uq})}{2} (C_{\ell,\text{in}}^{EE} - C_{\ell,\text{in}}^{BB}),$$

$$\widehat{C}_\ell^{TB} \simeq \frac{m_{ii}(m_{qq} - m_{uu})}{2} C_{\ell,\text{in}}^{TB} - \frac{m_{ii}(m_{qu} + m_{uq})}{2} C_{\ell,\text{in}}^{TE}.$$

analytical vs non-ideal output spectra



impact on cosmic birefringence

HWP-induced miscalibration

Analytic \hat{C}_ℓ s satisfy the relations:

$$\begin{cases} \hat{C}_\ell^{EB} \simeq \tan(4\hat{\theta}) \left[\hat{C}_\ell^{EE} - \hat{C}_\ell^{BB} \right] / 2 \\ \hat{C}_\ell^{TB} \simeq \tan(2\hat{\theta}) \hat{C}_\ell^{TE} \end{cases}$$

The HWP induces an additional miscalibration,
degenerate with cosmic birefringence and polarization angle
miscalibration!

HWP-induced miscalibration

Analytic \hat{C}_ℓ s satisfy the relations:

$$\begin{cases} \hat{C}_\ell^{EB} \simeq \tan(4\hat{\theta}) \left[\hat{C}_\ell^{EE} - \hat{C}_\ell^{BB} \right] / 2 \\ \hat{C}_\ell^{TB} \simeq \tan(2\hat{\theta}) \hat{C}_\ell^{TE} \end{cases} \quad \hat{\theta} \equiv -\frac{1}{2} \arctan \frac{m_{qu} + m_{uq}}{m_{qq} - m_{uu}} \sim 3.8^\circ,$$

our formulae suggest

compatibly with simulations.

The HWP induces an additional miscalibration,
degenerate with cosmic birefringence and polarization angle
miscalibration!

This doesn't mean that the HWP will keep us from measuring β ,
but it shows how important it is to carefully calibrate \mathcal{M}_{HWP} .

simple generalizations

including frequency dependence

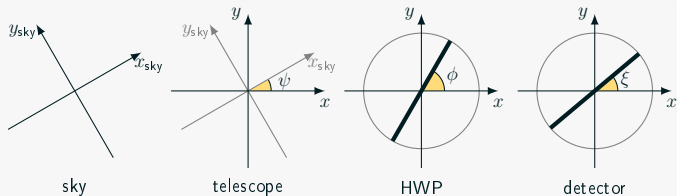
How does $d = (1 \ 0 \ 0) \cdot \mathcal{M}_{\text{det}} \mathcal{R}_{\xi-\phi} \mathcal{M}_{\text{HWP}} \mathcal{R}_{\phi+\psi} \cdot \mathbf{S}$ change when the **frequency dependence** of \mathcal{M}_{HWP} and signal is taken into account?

$$d = (1 \ 0 \ 0) \cdot \mathcal{M}_{\text{det}} \mathcal{R}_{\xi-\phi} \int d\nu \mathcal{M}_{\text{HWP}}(\nu) \mathcal{R}_{\phi+\psi} \cdot \mathbf{S}(\nu).$$

Assuming an ideal map-maker and retracing the same steps as before:

$$\hat{\theta} = -\frac{1}{2} \arctan \frac{\langle m_{qu} + m_{uq} \rangle}{\langle m_{qq} - m_{uu} \rangle}, \quad \text{where } \langle \cdot \rangle = \int d\nu \cdot (\nu) S(\nu).$$

instrument miscalibration



So far, we assumed $\begin{cases} \hat{\psi} \equiv \psi, \\ \hat{\phi} \equiv \phi, \\ \hat{\xi} \equiv \xi, \end{cases}$ but more generally $\begin{cases} \hat{\psi} \equiv \psi + \delta\psi, \\ \hat{\phi} \equiv \phi + \delta\phi, \\ \hat{\xi} \equiv \xi + \delta\xi. \end{cases}$

Taking such (frequency-independent) deviations into account:

$$\hat{\theta} = -\frac{1}{2} \arctan \frac{\langle m_{qu} + m_{uq} \rangle}{\langle m_{qq} - m_{uu} \rangle} + \delta\theta, \quad \text{where } \delta\theta \equiv \delta\xi - \delta\psi - 2\delta\phi.$$

steps forward

Even *more general* generalizations worth exploring:

including a realistic band pass,

allowing for miscalibrations to depend on ν .

For how long can we push the analytical formulae?

the importance of calibration

how does the map-model change

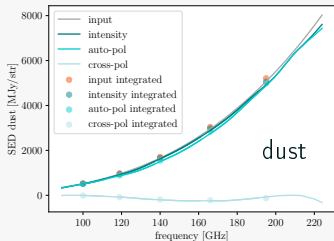
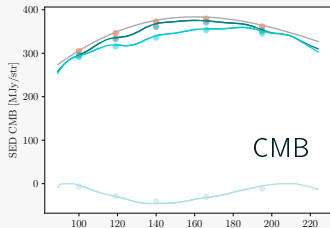
Without HWP:
$$\begin{pmatrix} I_j \\ Q_j \\ U_j \end{pmatrix} = \sum_{\lambda} g_{\lambda} \begin{pmatrix} I_{\lambda} \\ Q_{\lambda} \\ U_{\lambda} \end{pmatrix} + n,$$

With HWP:
$$\begin{pmatrix} I_j \\ Q_j \\ U_j \end{pmatrix} = \sum_{\lambda} \begin{pmatrix} g_{\lambda}^{ii} & 0 & 0 \\ 0 & g_{\lambda}^{qq-uu} & g_{\lambda}^{qu+uq} \\ 0 & g_{\lambda}^{qu+uq} & g_{\lambda}^{qq-uu} \end{pmatrix} \begin{pmatrix} I_{\lambda} \\ Q_{\lambda} \\ U_{\lambda} \end{pmatrix} + n,$$

where $g_{\lambda} = \frac{\int d\nu G(\nu) S_{\lambda}(\nu)}{\int d\nu G(\nu)}$, $g_{\lambda}^{ii} = \frac{\int d\nu G(\nu) m_{ii}(\nu) S_{\lambda}(\nu)}{\int d\nu G(\nu)}$, and so on.

HWP non-idealities contribute to **gain**, **polarization-efficiency**
and **cross-polarization leakage**.

effective SEDs



$$\sum_{\lambda} \begin{pmatrix} g_{\lambda}^{ii} & 0 & 0 \\ 0 & g_{\lambda}^{qq-uu} & g_{\lambda}^{qu+uq} \\ 0 & g_{\lambda}^{qu+uq} & g_{\lambda}^{qq-uu} \end{pmatrix} \begin{pmatrix} I_{\lambda} \\ Q_{\lambda} \\ U_{\lambda} \end{pmatrix} + n,$$

Since all these effects are frequency dependent, they affect each component differently,

An imprecise calibration of \mathcal{M}_{HWP} can lead to complications in the component separation step.

we are now provided with a **simulation pipeline** that can be easily adapted to study more complex problems (adding noise, more realistic beams...);

the **analytical formulae** represent an alternative tool to study the same problems more effectively (but approximately);

obvious application: exploiting the analytical formulae to derive **calibration requirements** for the HWP Mueller matrix elements, so that they don't prevent us from detecting ***B*-modes**, measuring **cosmic birefringence**, nor spoil the **foreground cleaning** procedure.